Journal of Sound and Vibration (1997) **203**(4), 547–561

THE STEELPAN AS A SYSTEM OF NON-LINEAR MODE-LOCALIZED OSCILLATORS, PART II: COUPLED SUB-SYSTEMS, SIMULATIONS AND EXPERIMENTS

A. Achong and K. A. Sinanan-Singh

Department of Physics, University of the West Indies, St. Augustine, Trinidad, West Indies

(*Received* 26 *June* 1996, *and in final form* 25 *November* 1996)

This paper is a sequel to reference [1]. In that paper, the dynamics of the steelpan notes were developed as systems of non-linear mode-localized oscillators. The present paper examines the coupled note-note and note-skirt systems on the steelpan modelled as a plexus of non-linear oscillators interconnected by linear mechanical filters. The tonal qualities of a note depend on the degree of coupling and the closeness in frequency of the excited modes on the interacting subsystems. Modes above the fundamental (the partials) are produced by internal and combination resonances.

1. INTRODUCTION

In an earlier paper [1] (hereafter referred to as Part I), the first author described the physical structure of the steelpan and examined the response of the notes to impacts produced by striking the notes with the stick (mallet). Each note was modelled as a non-linear system for which the governing equations for note vibrations contained only linear and quadratic terms. The vibrations on these notes are confined to an elliptically shaped area of the note [2]. The exchange of energy between resonances on a note produces amplitude as well as frequency modulations.

Situations always arise on the steelpan where the mechanical coupling between subsystems (notes and skirt) is important. When the pan is being tuned for example, some notes may, by chance, have almost the same fundamental frequency as the desired frequency of the note to be tuned. The coupling of these notes makes it extremely difficult for the panmaker to tune the note. Coupling between note and skirt produces a similar difficulty. In the latter case the coupling remains after tuning is completed and this degrades the tonal quality.

For a fuller discussion on the steelpan and non-linearities found on other instruments the reader should consult Part I and the reference contained therein.

2. THEORETICAL DEVELOPMENT

2.1. THE COMBINATORICS AND BASIC PROPERTIES OF THE SYSTEM

Consider the system of N-connected domains $\Omega_1, \Omega_2, \ldots, \Omega_N$ (see Figure 1). All of these domains, except one (on the steelpan, the cylindrical skirt), are of similar geometry (describing the shallow cap-like notes) but they differ in geometrical details (size, rise etc.) and in elastic properties. The domains are connected by means of elastic elements (defined

0022–460X/97/240547 + 15 $25.00/0/sv960873

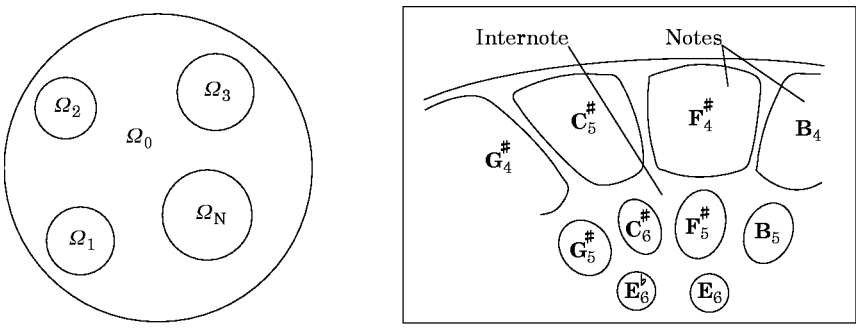

(a) (b)

Figure 1. (a) the $N + 1$ domains of the system; (b) a section of a typical tenor steelpan.

in this paper as *internotes*, for panmakers have not yet found a term for these pan elements) represented by the panface exclusive of the notes. The connection of *internotes* form the domain Ω_0. All notes are considered to be non-linear systems while the physically largest element, the skirt, is modelled linearly.

The transmission conditions which describe processes in Ω_0, as influenced by the N domains, are assumed to produce linear paths connecting the N domains. On the steelpan, this condition of linearity is made possible by the process of hammering the *internotes* to produce a stiffened plate with resonant frequencies higher than those of the notes. In this way, the *internotes* are made to function as linear mechanical filters at the note frequencies. Electronically, the steelpan can be modelled as a plexus of non-linear oscillators interconnected by R-C filters.

2.2. THE DYNAMICS OF THE SYSTEM

In considering the vibrations of the sub-systems of the steelpan, the work of Part I is extended to include the two most frequently encountered cases of domain interaction on the properly constructed pan: (1) two-domain note–note interaction and (2) two-domain note–skirt interaction. At any time, in any one of these interactions, one domain may be regarded as the receiver and the other as the source. The roles of source and receiver are interchangeable.

As in Part I, only quadratic non-linearities are considered and they appear, in the system of equations, to the first order in the gauge parameter ε. A cubic term (if mid-surface stretching is included) would be to second order in ε.

There are two sets of quadratic terms to consider. The first of these contain products describing interactions between components of the same domain (the α-terms) and those describing the non-linear interaction between the source and receiver domains (the β-terms). There will also be terms describing linear interactions between the two domains (the Γ-terms). The spatial separation of the two domains requires the introduction of complex coupling coefficients $\boldsymbol{\beta} = \beta\, e^{i\beta}$ and $\boldsymbol{\Gamma} = \Gamma\, e^{i\delta}$ to account for the phase shifts produced on transmission across the connecting domain Ω_0.

On a 3-D system such as the steelpan there is, in general, the possibility of multiple paths between source and receiver, with each path producing its own amplitude- and phase-modified signal at the receiving domain. These multiple paths would be of particular importance during and immediately following the initial transient produced by the stick impact. Since however, the typical dimension (L) of any substructure (domain) on the pan satisfies the condition $L \ll c/f$ (where c is the sound velocity in steel and f is the signal

frequency), while the note is sounding, a single pair of phase and amplitude values may be used to describe the resultant signal for each frequency component arriving at the receiver domain.

The notes on a steelpan are excited by stick (hammer) impact which produces a short duration *impact phase* followed by a longer duration *free vibration phase* [1]. As in Part I, the transverse vibration displacement fields on domain d can be expressed in a form separable in space and time as

$$W_d(\mathbf{r}, t) = \sum_{n=1}^{\infty} u_{nd}(t) V_{nd}(\mathbf{r}),$$

where $V_{nd}(\mathbf{r})$ are appropriate spatial functions (mode shapes) satisfying the boundary conditions of the domain, n is the mode number, and $u_{nd}(t)$ are unknown functions of time only. Solutions are sought for the component $u_{nd}(t)$ on the coupled system using a version of equation (2) of Part I modified to include domain–domain coupling. The governing equations are

$$\ddot{u}_{nd} + \omega_{nd}^2 u_{nd} + \varepsilon\Bigg[2\mu_{nd}\dot{u}_{nd} - \sum_{j=1}^{\infty}\sum_{k=1}^{\infty} \alpha_{jkn}^{\{d\}} u_{jd} u_{kd} - \sum_{j=1}^{\infty}\sum_{k=1}^{\infty}\sum_{p=1}^{2} \beta_{jp,k\bar{p}}^{\{nd\}} u_{jp} u_{k\bar{p}}$$

$$- \sum_{j=1}^{\infty} \Gamma_{j\bar{d}}^{\{nd\}} u_{j\bar{d}} - f_d(t)\Bigg] = 0, \tag{1}$$

where d defines the source domain and $\bar{d}$ the receiver domain ($\bar{d} = 1(2)$ when $d = 2(1)$); $\bar{p} = 1(2)$ when $p = 2(1)$; u_{nd} are the displacements; the dots refer to differentiation with respect to time t; ω_{nd} are the natural frequencies of the linearized subsystems with $\omega_{1d} < \omega_{2d}, \ldots, < \omega_{\infty d}$; μ_{nd} are the damping coefficients; $\alpha_{jkn}^{\{d\}}$ are constants with $\alpha_{jkn}^{\{d\}} = \alpha_{kjn}^{\{d\}}$; $f_d(t)$ is a short duration external impulse which is set to zero after impact for the free system.

In the multi-time scale procedure [3, 4], one defines $t_0 = t$, $t_1 = \varepsilon t$, where the main oscillatory behaviour occurring at frequencies ω_n are associated with the fast time scale t_0, while amplitude and phase modulations due to damping and non-linearities take place on the slow time scale t_1. Also, the time derivative is $\mathrm{d}/\mathrm{d}t = D_0 + \varepsilon D_1$ where $D_n = \partial/\partial t_n$. The procedure allows the independent variable u_n to be expanded in the form $u_{nd} = u_{n0d}(t_0, t_1) + \varepsilon u_{n1d}(t_0, t_1) + O(\varepsilon^2)$. By substituting this equation into equation (1), transforming time derivatives and equating coefficients of like powers of ε, one obtains the following set of equations for the coupled note-note or note-skirt system during the free vibration phase:

order ε^0,

$$D_0^2 u_{n0d} + \omega_{nd}^2 u_{n0d} = 0; \tag{2}$$

order ε^1,

$$D_0^2 u_{n1d} + \omega_n^2 u_{n1d} = -2D_0(D_1 + \mu_{nd}) u_{n0d} + \sum_{j=1}^{\infty}\sum_{k=1}^{\infty} \alpha_{jkn}^{\{d\}} u_{j0d} u_{k0d}$$

$$+ \sum_{j=1}^{\infty}\sum_{k=1}^{\infty}\sum_{p=1}^{2} B_{jp,k\bar{p}}^{\{nd\}} u_{j0p} u_{k0\bar{p}} + \sum_{j=1}^{\infty} \Gamma_{j\bar{d}}^{\{nd\}} u_{j0\bar{d}}. \tag{3}$$

The general solution of equation (2) takes the form $u_{n0d} = A_{nd}(t_1)\,e^{i\omega_{nd}t_0} + CC$ where $A_{nd} = \frac{1}{2}a_{nd}\,e^{i\phi_{nd}}$ with a_{nd} and ϕ_{nd} being functions of the slow time t_1 and representing the amplitude and phase of the nth Fourier component of the displacement, respectively.

2.2.1. *Case* 1: *note–note interaction*

The interacting pair of notes of importance on the steelpan is the combination of an outer note and an inner note tuned to the upper octave (refer to Figure 1(b) where the pairs $\{\mathbf{B}_4; \mathbf{B}_5\}$ and $\{\mathbf{F}_4^{\#}; \mathbf{F}_5^{\#}\}$, for example, can be identified). These neighbouring notes are usually tuned to operate in "sympathetic" vibration, with the upper octave acting as the "second harmonic" when the lower octave is played. On some steelpans, note pairs of this type can be found that are almost entirely dependent on note–note coupling for tonal quality and structure. In the system of equations governing the coupled pair of notes, the note of lower frequency (domain 1) is described as a 3-DOF system, and the higher note (domain 2) as a 2-DOF system. This is a sufficient description, as the third mode on the higher note and the fourth mode on the lower note have been observed on most steelpans to be very low in amplitude and will therefore produce relatively weak interaction products in combination resonances.

The resonances studied here, correspond in domain 1 to an internal resonance with $\omega_{21} \approx 2\omega_{11}$, a combination resonance with $\omega_{31} \approx \omega_{11} + \omega_{21}$, and in domain 2 to internal resonances with $\omega_{12} \approx 2\omega_{11}$ and $\omega_{22} \approx 2\omega_{12}$. The closeness of these resonances are described by the detuning parameters σ_1, σ_2, σ_3 and σ_4, where

$$\omega_{21} = 2\omega_{11} + \varepsilon\sigma_1, \qquad \omega_{31} = \omega_{11} + \omega_{21} + \varepsilon\sigma_2,$$
$$\omega_{12} = 2\omega_{11} + \varepsilon\sigma_3, \qquad \omega_{22} = 2\omega_{12} + \varepsilon\sigma_4. \tag{4}$$

The solvability conditions are obtained from equations (2) to (4) by the procedure outlined in Part I. The separation of real and imaginary parts convert these solvability equations to

$$a_{11}' = -\mu_{11}a_{11} + \frac{\alpha_{121}^{\{1\}*}}{4\omega_{11}}a_{11}a_{21}\sin\gamma_1 + \frac{\alpha_{231}^{\{1\}*}}{4\omega_{11}}a_{21}a_{31}\sin\gamma_2 + \frac{\beta_{12,11}^{\{11\}}}{4\omega_{11}}a_{12}a_{11}\sin(\gamma_1+\gamma_3+\theta_\beta)$$
$$+ \frac{\beta_{12,31}^{\{11\}}}{4\omega_{11}}a_{12}a_{31}\sin(\gamma_2-\gamma_3+\theta_\beta) + \frac{\beta_{22,31}^{\{11\}}}{4\omega_{11}}a_{22}a_{31}\sin(\gamma_5+\theta_\beta),$$

$$a_{21}' = -\mu_{21}a_{21} - \frac{\alpha_{112}^{\{1\}}}{4\omega_{21}}a_{11}^2\sin\gamma_1 + \frac{\alpha_{132}^{\{1\}*}}{4\omega_{21}}a_{11}a_{31}\sin\gamma_2 + \frac{\beta_{21,22}^{\{21\}}}{4\omega_{21}}a_{21}a_{22}\sin(2\gamma_3+\gamma_4+\theta_\beta)$$
$$+ \frac{\beta_{22,12}^{\{21\}}}{4\omega_{21}}a_{22}a_{12}\sin(\gamma_3+\gamma_4-\theta_\beta) + \frac{\Gamma_{12}^{\{21\}}}{2\omega_{21}}a_{12}\sin(\gamma_3+\delta_\Gamma),$$

$$a_{31}' = -\mu_{31}a_{31} - \frac{\alpha_{123}^{\{1\}*}}{4\omega_{31}}a_{11}a_{21}\sin\gamma_2 + \frac{\beta_{12,11}^{\{31\}}}{4\omega_{31}}a_{12}a_{11}\sin(\gamma_3-\gamma_2+\theta_\beta)$$
$$+ \frac{\beta_{22,11}^{\{31\}}}{4\omega_{31}}a_{22}a_{11}\sin(\gamma_5+\theta_\beta),$$

$$\phi_{11}' = -\frac{\alpha_{121}^{\{1\}*}}{4\omega_{11}}a_{21}\cos\gamma_1 - \frac{\alpha_{231}^{\{1\}*}}{4\omega_{11}}\frac{a_{21}a_{31}}{a_{11}}\cos\gamma_2 - \frac{\beta_{12,11}^{\{11\}}}{4\omega_{11}}a_{12}\cos(\gamma_1+\gamma_3+\theta_\beta)$$
$$- \frac{\beta_{12,31}^{\{11\}}}{4\omega_{11}}\frac{a_{12}a_{31}}{a_{11}}\cos(\gamma_2-\gamma_3+\theta_\beta) - \frac{\beta_{22,31}^{\{11\}}}{4\omega_{11}}\frac{a_{22}a_{31}}{a_{11}}\cos(\gamma_5+\theta_\beta),$$

$$\phi'_{21} = -\frac{\alpha^{\{1\}}_{112}}{4\omega_{21}}\frac{a_{11}^2}{a_{21}}\cos\gamma_1 - \frac{\alpha^{\{1\}^*}_{132}}{4\omega_{21}}\frac{a_{11}a_{31}}{a_{21}}\cos\gamma_2 - \frac{\beta^{\{21\}}_{21,22}}{4\omega_{21}}a_{22}\cos(2\gamma_3+\gamma_4+\theta_\beta)$$
$$-\frac{\beta^{\{21\}}_{22,12}}{4\omega_{21}}\frac{a_{22}a_{12}}{a_{21}}\cos(\gamma_3+\gamma_4+\theta_\beta) - \frac{\Gamma^{\{21\}}_{12}}{2\omega_{21}}\frac{a_{12}}{a_{21}}\cos(\gamma_3+\delta_\Gamma),$$

$$\phi'_{31} = -\frac{\alpha^{\{1\}^*}_{123}}{4\omega_{31}}\frac{a_{11}a_{21}}{a_{31}}\cos\gamma_2 - \frac{\beta^{\{31\}}_{12,11}}{4\omega_{31}}\frac{a_{12}a_{11}}{a_{31}}\cos(\gamma_3-\gamma_2+\theta_\beta) - \frac{\beta^{\{31\}}_{22,11}}{4\omega_{31}}\frac{a_{22}a_{11}}{a_{31}}\cos(\gamma_5+\theta_\beta),$$

$$a'_{12} = -\mu_{12}a_{12} + \frac{\alpha^{\{2\}^*}_{121}}{4\omega_{12}}a_{12}a_{22}\sin\gamma_4 + \frac{\beta^{\{12\}}_{31,11}}{4\omega_{12}}a_{31}a_{11}\sin(\gamma_2-\gamma_3+\theta_\beta)$$
$$+\frac{\beta^{\{12\}}_{22,21}}{4\omega_{12}}a_{22}a_{21}\sin(\gamma_3+\gamma_4+\theta_\beta) - \frac{\beta^{\{12\}}_{11,11}}{4\omega_{12}}a_{11}^2\sin(\gamma_1+\gamma_3+\theta_\beta) - \frac{\Gamma^{\{12\}}_{21}}{2\omega_{12}}a_{21}\sin(\gamma_3+\theta_\beta),$$

$$a'_{22} = -\mu_{22}a_{22} - \frac{\alpha^{\{2\}}_{112}}{4\omega_{22}}a_{12}^2\sin\gamma_4 - \frac{\beta^{\{22\}}_{31,11}}{4\omega_{22}}a_{31}a_{11}\sin(\gamma_5+\theta_\beta) - \frac{\beta^{\{22\}}_{21,21}}{4\omega_{22}}a_{21}^2\sin(2\gamma_3+\gamma_4+\theta_\beta)$$
$$-\frac{\beta^{\{22\}}_{21,12}}{4\omega_{22}}a_{21}a_{12}\sin(\gamma_3+\gamma_4+\theta_\beta),$$

$$\phi'_{12} = -\frac{\alpha^{\{2\}^*}_{121}}{4\omega_{12}}a_{22}\cos\gamma_4 - \frac{\beta^{\{12\}}_{31,11}}{4\omega_{12}}\frac{a_{31}a_{11}}{a_{12}}\cos(\gamma_5+\theta_\beta) - \frac{\beta^{\{12\}}_{11,11}}{4\omega_{12}}\frac{a_{11}^2}{a_{12}}\cos(\gamma_1+\gamma_3+\theta_\beta)$$
$$-\frac{\beta^{\{12\}}_{22,21}}{4\omega_{12}}\frac{a_{22}a_{21}}{a_{12}}\cos(\gamma_3+\gamma_4+\theta_\beta) - \frac{\Gamma^{\{12\}}_{21}}{2\omega_{12}}\frac{a_{21}}{a_{12}}\cos(\gamma_3+\delta_\Gamma),$$

$$\phi'_{22} = -\frac{\alpha^{\{2\}}_{112}}{4\omega_{22}}\frac{a_{12}^2}{a_{22}}\cos\gamma_4 - \frac{\beta^{\{22\}}_{31,11}}{4\omega_{22}}\frac{a_{31}a_{11}}{a_{22}}\cos(\gamma_5+\theta_\beta) - \frac{\beta^{\{22\}}_{21,21}}{4\omega_{22}}\frac{a_{21}^2}{a_{22}}\cos(2\gamma_3+\gamma_4+\theta_\beta)$$
$$-\frac{\beta^{\{22\}}_{21,12}}{4\omega_{22}}\frac{a_{21}a_{12}}{a_{22}}\cos(\gamma_3+\gamma_4+\theta_\beta), \tag{5a–j}$$

where the prime denotes $\mathrm{d}/\mathrm{d}t_1$; θ_β and δ_Γ represent the phase angles corresponding to the β and Γ coefficients in each term; $\alpha^{\{d\}^*}_{jkn} = \alpha^{\{d\}}_{jkn} + \alpha^{\{d\}}_{kjn}$; and

$$\gamma_1 = \phi_{21} - 2\phi_{11} + \sigma_1 t_1, \qquad \gamma_2 = \phi_{31} - \phi_{21} - \phi_{11} + \sigma_2 t_1, \qquad \gamma_3 = \phi_{12} - \phi_{21} + (\sigma_3 - \sigma_1)t_1,$$
$$\gamma_4 = \phi_{22} - 2\phi_{12} + \sigma_4 t_1, \qquad \gamma_5 = \gamma_1 - \gamma_2 + 2\gamma_3 + \gamma_4. \tag{6a–e}$$

Varying the values in the parameter set $(\omega, \mu, \sigma, \alpha, \beta, \Gamma)$ allows the full range of modulation features to be observed on the coupled note–note system to be modelled mathematically.

2.2.2. *Case* 2: *note-skirt interactions*

A case often encountered on the pan is the interaction between the note being played and the skirt. When this occurs, it is usually the case that a single excited mode on the skirt will interact with the note. Overcoupling however can have undesirable effects as the tonal quality of the note is lost.

The skirt when left at its full un-cut length for the lower frequency pans (the bass instruments), is a cylindrical shell with two circumferential ridges (see Figure 2). These ridges serve as stiffeners on the original steel drum. As if by design, these stiffened cylindrical shells were "made to order" for this instrument. Because of the stiffeners, high frequencies will excite "local" modes in which vibration occurs predominantly in a small section of the stiffened cylinder. This tends to reduce note-skirt coupling in many cases.

Two resonances, corresponding to the second and third non-linear modes, are considered for the note (domain 1, modelled as a 3-DOF system). At the levels of excitation

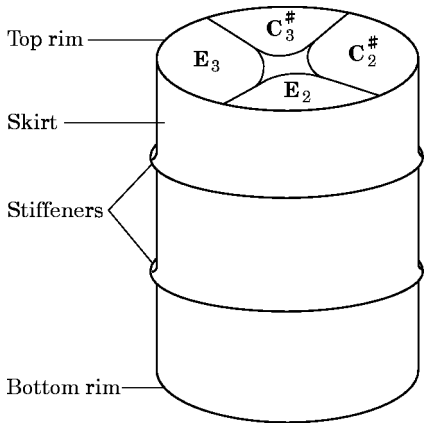

Figure 2. Sketch of a typical bass pan. Skirt length = 88 cm, diameter = 57 cm.

attained on the pan while being played, no non-linear effects have been detected experimentally on the skirt. A single, linear mode, is therefore considered for the skirt (domain 2, modelled as a 1-DOF system). To express quantitatively the nearness of these resonances one defines the detuning parameters σ_1, σ_2 and σ_3 according to

$$\omega_{21} = 2\omega_{11} + \varepsilon\sigma_1, \qquad \omega_{31} = \omega_{11} + \omega_{21} + \varepsilon\sigma_2, \qquad \omega_{12} = \omega_1 + \varepsilon\sigma_3. \tag{7a–c}$$

Applying these conditions to the system equations yields the following solvability equations:

$$\begin{aligned}
a'_{11} &= -\mu_{11}a_{11} + \frac{\alpha^{\{1\}*}_{121}}{4\omega_{11}}a_{11}a_{21}\sin\gamma_1 + \frac{\alpha^{\{1\}*}_{231}}{4\omega_{11}}a_{21}a_{31}\sin\gamma_2 + \frac{\beta^{\{11\}}_{12,21}}{4\omega_{11}}a_{12}a_{21}\sin(\gamma_1 - \gamma_3 + \theta_\beta)\\
&\quad + \frac{\Gamma^{\{11\}}_{12}}{2\omega_{11}}a_{12}\sin(\gamma_3 + \delta_\Gamma),\\
a'_{21} &= -\mu_{21}a_{21} - \frac{\alpha^{\{1\}}_{112}}{4\omega_{21}}a_{11}^2\sin\gamma_1 + \frac{\alpha^{\{1\}*}_{132}}{4\omega_{21}}a_{11}a_{31}\sin\gamma_2 - \frac{\beta^{\{21\}}_{12,11}}{4\omega_{21}}a_{12}a_{11}\sin(\gamma_1 - \gamma_3 + \theta_\beta),\\
a'_{31} &= -\mu_{31}a_{31} - \frac{\alpha^{\{1\}*}_{123}}{4\omega_{31}}a_{11}a_{21}\sin\gamma_2 + \frac{\beta^{\{31\}}_{12,21}}{4\omega_{31}}a_{12}a_{21}\sin(\gamma_3 - \gamma_2 + \theta),\\
\phi'_{11} &= -\frac{\alpha^{\{1\}*}_{121}}{4\omega_{11}}a_{21}\cos\gamma_1 - \frac{\alpha^{\{1\}*}_{231}}{4\omega_{11}}\frac{a_{21}a_{31}}{a_{11}}\cos\gamma_2 - \frac{\beta^{\{11\}}_{12,21}}{4\omega_{11}}\frac{a_{12}a_{21}}{a_{11}}\cos(\gamma_1 - \gamma_3 + \theta_\beta)\\
&\quad - \frac{\Gamma^{\{11\}}_{12}}{2\omega_{11}}\frac{a_{12}}{a_{11}}\cos(\gamma_3 + \delta_\Gamma),\\
\phi'_{21} &= -\frac{\alpha^{\{1\}}_{112}}{4\omega_{21}}\frac{a_{11}^2}{a_{21}}\cos\gamma_1 - \frac{\alpha^{\{1\}*}_{132}}{4\omega_{21}}\frac{a_{11}a_{31}}{a_{21}}\cos\gamma_2 - \frac{\beta^{\{21\}}_{12,12}}{4\omega_{21}}\frac{a_{12}^2}{a_{21}}\cos(2\gamma_3 - \gamma_1 + \theta_\beta)\\
&\quad - \frac{\beta^{\{21\}}_{12,11}}{4\omega_{21}}\frac{a_{12}a_{11}}{a_{21}}\cos(\gamma_1 - \gamma_3 + \theta_\beta),\\
\phi'_{31} &= -\frac{\alpha^{\{1\}*}_{123}}{4\omega_{31}}\frac{a_{11}a_{21}}{a_{31}}\cos\gamma_2 - \frac{\beta^{\{31\}}_{12,21}}{4\omega_{31}}\frac{a_{12}a_{21}}{a_{31}}\cos(\gamma_3 - \gamma_2 + \theta_\beta),\\
a'_{12} &= -\mu_{12}a_{12} - \frac{\Gamma^{\{12\}}_{11}}{2\omega_{12}}a_{11}\sin(\gamma_3 + \delta_\Gamma), \qquad \phi'_{12} = -\frac{\Gamma^{\{12\}}_{11}}{2\omega_{12}}\frac{a_{11}}{a_{12}}\cos(\gamma_3 + \delta_\Gamma),
\end{aligned} \tag{8a–h}$$

where

$$\gamma_1 = \phi_{21} - 2\phi_{11} + \sigma_1 t_1, \qquad \gamma_2 = \phi_{31} - \phi_{21} - \phi_{11} + \sigma_2 t_1, \qquad \gamma_3 = \phi_{12} - \phi_{11} + \sigma_3 t_1. \quad (9a–c)$$

3. EXPERIMENTAL AND COMPUTATIONAL METHODS

The methods for data acquisition and note excitation are the same as those described in Part I. Two velocity transducers were used, however, to simultaneously monitor each of the two interacting regions. Two sets of data were acquired for each note-note pair by exciting each note, in turn, by stick impacts. For the note-skirt interaction, impacts were applied only to the note. The velocity data were analyzed using the Short-Time Fourier Transform (STFT) with the Gaussian window set as in Part I and the corresponding displacement amplitudes and phases deduced from the transformed velocity data. The nth Fourier component in domain d is represented by S_{nd}. As shown in Part I, the multi-time analysis can be compared with the experimental data through the "equivalence" $a_{nd} \equiv |S_{nd}|$ and $\phi_{nd} \equiv \arg(S_{nd})$.

Equations (5a–j) and (8a–h) were integrated numerically using a fourth order Runge–Kutta routine to produce discretized values for a_{nd} and ϕ_{nd} at time steps of 0·1.

4. RESULTS AND DISCUSSION

4.1. NUMERICAL AND EXPERIMENTAL RESULTS

Following the procedure in Part I, the stick impacts were tabulated in the musical manner from "very soft" (*pianissimo*) to "loud" (*forte*) as judged from the acoustical level of the tone.

All numerical computations on the equation system (5a–j) and (8a–h) were done with parameter values chosen to closely (but not necessarily exactly) model the tones produced on the pan.

4.2. THE BASS D_3 NOTE-SKIRT INTERACTION

Tone structures are shown for the $\mathbf{D}_3$ (146·8 Hz) note on a bass pan played at the *forte* level in Figure 3 and at the *piano* level in Figure 5. In both cases there are note-skirt interactions between the fundamental mode on the note and a mode of frequency 179 Hz which was found to be confined mainly to the lower third portion of the skirt between the lower stiffener and the bottom rim. To excite this mode on the skirt by striking the note on the panface, there had to be sufficiently strong coupling of this note to this subsection of the skirt.

4.2.1. *Forte level*

On a normal level of amplitude resolution (Figure 3(a)) there appears nothing unusual about the tone structure of this note. The non-linear interaction between the fundamental resonance corresponding to $\{nd\} = \{11\}$ and the internal resonance $\{nd\} = \{21\}$ show up as slow but pronounced modulations of the amplitudes S_{11} and S_{21} as the two modes constantly exchange energy. On the frequency plot (Figure 3(c)) one observes the corresponding low frequency modulations discussed in Part I.

Under higher resolution (Figure 3(b)), a faster low-level modulation is observed on the amplitude profile S_{11}. On the frequency plot Figure 3(c), the corresponding frequency modulation is quite significant. The frequency modulation on the fundamental mode is seen to grow steadily as the tone decays. The depth of frequency modulation

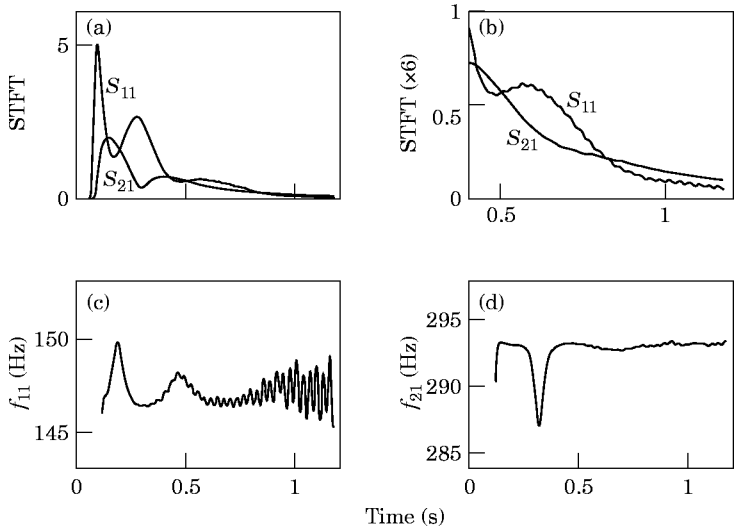

Figure 3. Experimental results for the bass $\mathbf{D}_3$ note played *forte* with skirt coupling: (a) displacement STFT, (b) STFT at higher resolution, (c) frequency modulation on f_{11} (= 146·9 + $\phi'/2\pi$ Hz), (d) frequency modulation on f_{21} (= 294·0 + $\phi'/2\pi$ Hz).

increases to as much as 2·5 Hz, representing a 1·7% change in frequency of the tone. While this surely represents significant changes in intonation, it occurs when the intensity of the tone has fallen to low levels. Nevertheless, this modulation was clearly audible as a warble, whenever the note was played. This warble could be stopped by clamping the lower rim of the skirt, clearly indicating that the effect was due to note-skirt coupling. There are no corresponding modulations of any significance on the higher modes.

The velocity STFT's were maximized at $f_{11} = 146{\cdot}9$ Hz (mode 1) and $f_{21} = 294$ Hz (mode 2).

This note-skirt system was modelled numerically and the results shown along with the frequency diagram in Figures 4(a–d). Modelling parameters were:

$\alpha_{211} = \alpha_{121} = 0{\cdot}0125$, $\alpha_{112} = 0{\cdot}025$, $\alpha_{123} = \alpha_{213} = 0{\cdot}015$, $\alpha_{132} = \alpha_{312} = 0{\cdot}005$, $\alpha_{231} = \alpha_{321} = 0{\cdot}01$, all $\beta = 0{\cdot}001$, $\Gamma_{12}^{\{11\}} = 0{\cdot}003$, $\Gamma_{11}^{\{12\}} = 0{\cdot}004$, $\mu_{11} = \mu_{21} = \mu_{31} = 0{\cdot}0006$, $\mu_{12} = 0{\cdot}0004$ $\sigma_1 = -0{\cdot}002$, $\sigma_2 = -0{\cdot}01$, $\sigma_3 = -0{\cdot}045$. Initial amplitudes where, *forte* level, $a_{11} = 1$, $a_{21} = a_{31} = 0$, $a_{12} = 0{\cdot}08$.

Observe the strong similarities in the details of the frequency diagrams obtained theoretically (Figure 4(a, c, d)) and experimentally (Figure 3(a, b, c)). The frequency modulation characteristics are properly reproduced in the mathematical synthesis. The non-linear domain-to-domain coupling constants $\beta_{jp,kp}^{\{nd\}}$ are quite small ($\beta = 0{\cdot}001$) resulting in an essentially linear note-skirt interaction.

The modulation which appears on the amplitude profile a_{11} (the theoretical equivalent to S_{11}) is described by the term $(\Gamma_{12}^{\{11\}}/2\omega_{11})a_{12}\sin(\gamma_3 + \delta_\Gamma)$ which appears in the expression for a'_{11} (equation (8a)). The angle γ_3 contains a term $(\omega_{12} - \omega_{11})t_1/\Theta$ which shows that the modulation is the result of a "beat" effect between the modes $\{nd\} = 11$ and $\{nd\} = \{12\}$ on a time-scale t_1 with angular frequency $|(\omega_{12} - \omega_{11})/\Theta|$.

The steady growth in the level of frequency modulation as the tone decays can be explained with the term $-(\Gamma_{12}^{\{11\}}/2\omega_{11})(a_{12}/a_{11})\cos(\gamma_3 + \delta_\Gamma)$ which appears in the expression for the frequency ϕ'_{11} (equation (8d)). Because of the long persistence of the skirt vibrations and the faster decay of the note vibrations (as an example, see Figure 7(a, c)),

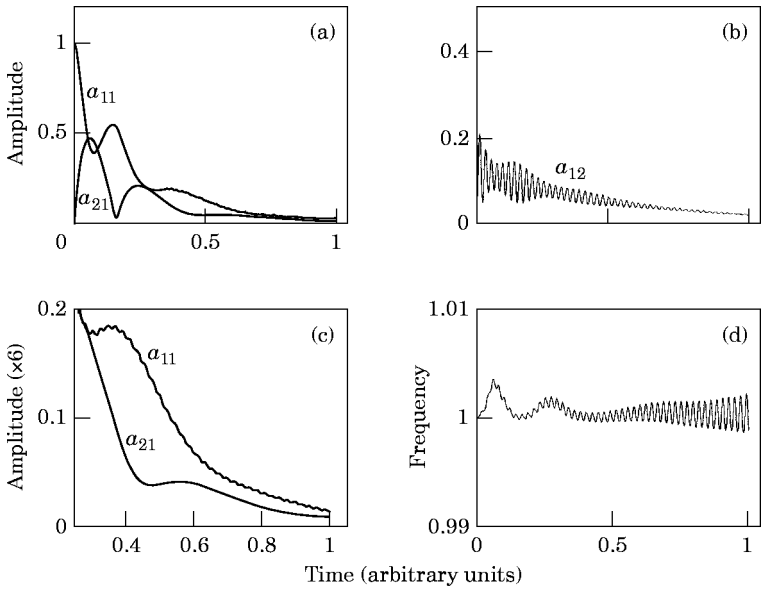

Figure 4. Analytical results for the simulated $\mathbf{D}_3$ note played *forte* with skirt coupling: (a) amplitudes of note components, (b) amplitude of skirt component, (c) note components under higher resolution, (d) frequency modulation on ω_{11} ($= 1 + \phi'_{11}$).

the amplitude ratio a_{12}/a_{11} actually increases as the tone decays, increasing the level of the frequency modulation. The cosine factor accounts for the periodicity.

4.2.2. *Piano level*

The experimental results for the $\mathbf{D}_3$ note excited at the *piano* level is shown in Figure 5, while in Figure 6 the numerically modelled note is shown for the same modelling

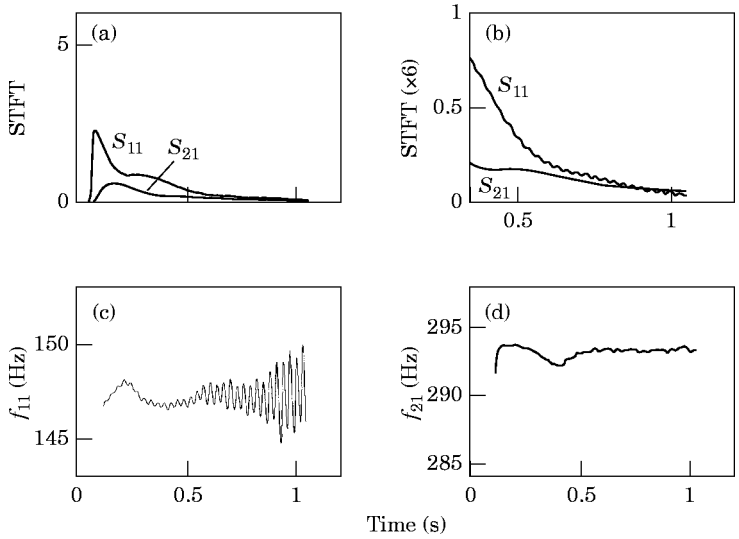

Figure 5. Experimental results for the bass $\mathbf{D}_3$ note played *piano* with skirt coupling: (a) displacement STFT, (b) STFT at higher resolution, (c) frequency modulation on f_{11} ($= 146{\cdot}9 + \phi'/2\pi$ Hz), (d) frequency modulation on f_{21} ($= 294{\cdot}0 + \phi'/2\pi$ Hz).

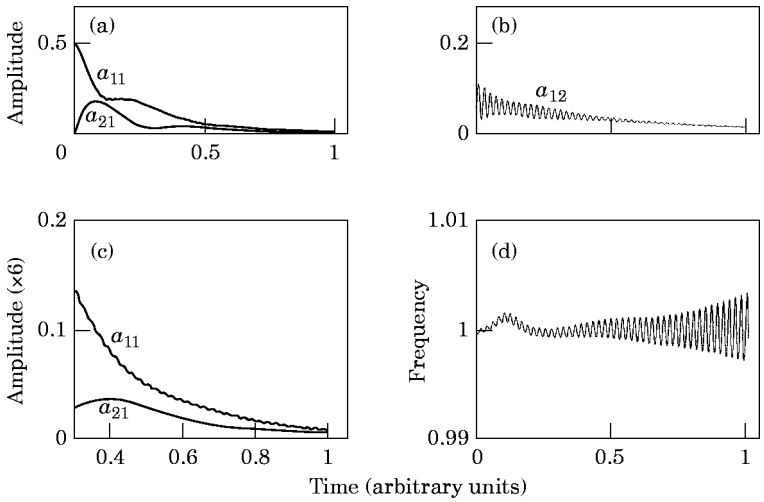

Figure 6. Analytical results for the simulated $\mathbf{D}_3$ note played *piano* with skirt coupling: (a) amplitudes of note components, (b) amplitude of skirt component, (c) note components under higher resolution, (d) frequency modulation on ω_{11} ($= 1 + \phi'_{11}$).

parameters used at the *forte* level but with initial amplitudes: $a_{11} = 0{\cdot}5$, $a_{21} = 0$, $a_{31} = 0$, $a_{12} = 0{\cdot}04$. Comparing Figures 5(a–c) with Figures 6(a, c, d), one finds that all the amplitude modulation and frequency modulation features for this note can be accounted for in the theory. One also observes that towards the end of the tone, the depth of frequency modulation on the fundamental mode ($\{nd\} = \{11\}$), produced by the note-skirt coupling, is greater when the note is played at the *piano* level than when it is played at the *forte* level. This is a direct result of the greater amplitude ratio a_{12}/a_{11} (or its equivalent S_{12}/S_{11}) expected in the dying stages of the tone in the former case.

In Part I it was shown that the tonal structure of the steelpan note is very dependent on the intensity of the impact, with a greater percentage of the energy going into the higher modes (the partials) when the note is played louder. With linear coupling between note and skirt it is now observed that the frequency modulation features produced by this coupling becomes more significant as the note is played softer.

4.3. THE $\mathrm{F}_3^{\#}$ NOTE ON A DOUBLE-SECOND STEELPAN

The "double-second" instrument consists of a pair of steelpans with notes of frequencies in the musical range $\mathbf{F}_3^{\#}$ (185·0 Hz) to $\mathbf{A}_5$ (880·0 Hz). The double-second tested, carried a skirt of length 25 cm, diameter 57 cm and sheet thickness 0·085 cm.

Figure 7 shows the time-histories and frequency spectra for the $\mathbf{F}_3^{\#}$ note and for the skirt on this instrument. Excitation was done using the stick and striking, in turn, the note and then the skirt. Figures 7(b) and 7(d) represent spectra for the velocity data so they show a high frequency emphasis (proportional to frequency) over the corresponding spectra for the displacements. The relative amplitudes of the components on the skirt spectra depend on time as well as the location of the transducer monitoring the motions of the skirt. Of immediate importance here is the much longer duration of the skirt excitation over that of the note and the near coincidence of the 186·0 Hz (fundamental) f_{11} component on the note and the 183·0 Hz (dominant) f_{12} component on the skirt.

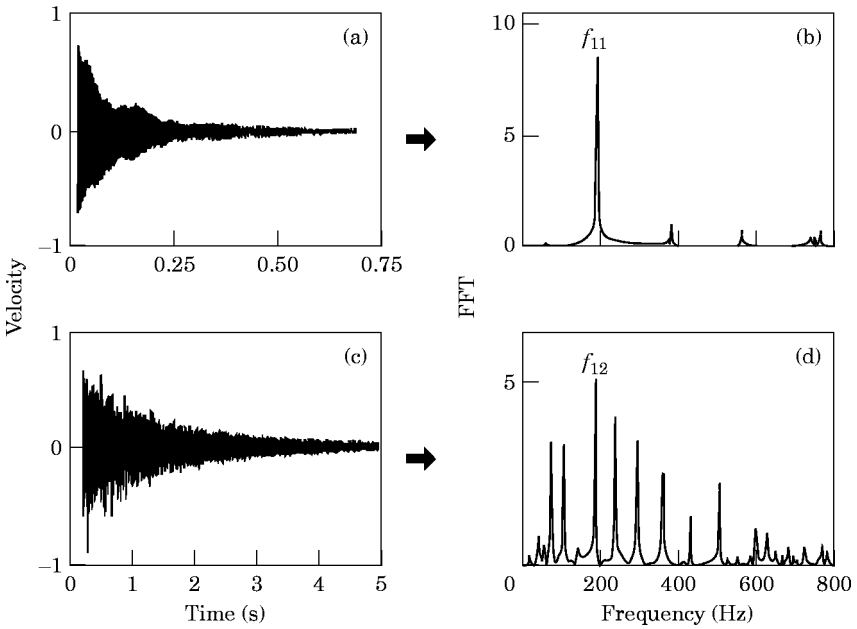

Figure 7. Experimental time histories and spectra for the $\mathbf{F}_3^{\#}$ note and the skirt on the double-second pan: (a) note time-history, (b) note spectrum, (c) skirt time-history, (d) skirt spectrum.

For the note played *forte*, Figure 8 shows the displacement amplitudes for three note components (S_{11}, S_{21}, and S_{31}) and for the 183 Hz component (S_{12}) of the skirt. The velocity data from which these results were computed were obtained by monitoring the note and the skirt simultaneously. There are some important features in these results which represent a case of strong note-skirt coupling.

In Figure 8(b), the skirt first responds to the impulse imparted directly to the note by the stick, with an initial rapid rise in displacement amplitude. This is followed at first by a short duration decay, then the motion is fed by the energy transferred from the note to the skirt. This transfer is accompanied by a rapid decay of the motion on the note (see Figure 8(a) where S_{11} decays rapidly). The decay on the note is halted somewhat as energy is transferred from the skirt back to the note, but decay continues until the amplitude of the first mode drops to almost zero after 0·6 s. Thereafter the motion of the note is controlled by energy transfers from the skirt.

Accompanying these amplitude modulation features are the changes in the frequency f_{11} of the fundamental mode on the note. Figure 8(d) shows the frequency (obtained from the time derivative of the phase ϕ_{11}) as it changes from a value varying around 186 Hz for the first 0·6 s to a value varying around 183 Hz (the value for the skirt component) for the remainder of the duration of the tone. This shows that the pumping action of the skirt on the note dominates the note dynamics after 0·6 s.

Of direct importance are the very low levels observed for both the internal resonance ($\omega_{21} \approx 2\omega_{11}$) and the combination resonance ($\omega_{31} \approx \omega_{11} + \omega_{21}$). Since these are the resonances that produce the partials on the steelpan, this note produces a rather dull tone. The fact that these resonances are observed at such low levels signify the absence of strong mode confinement—a result of the strong note-skirt coupling. Mode confinement, necessary on the steelpan for the tonal quality of the instrument, can therefore be destroyed

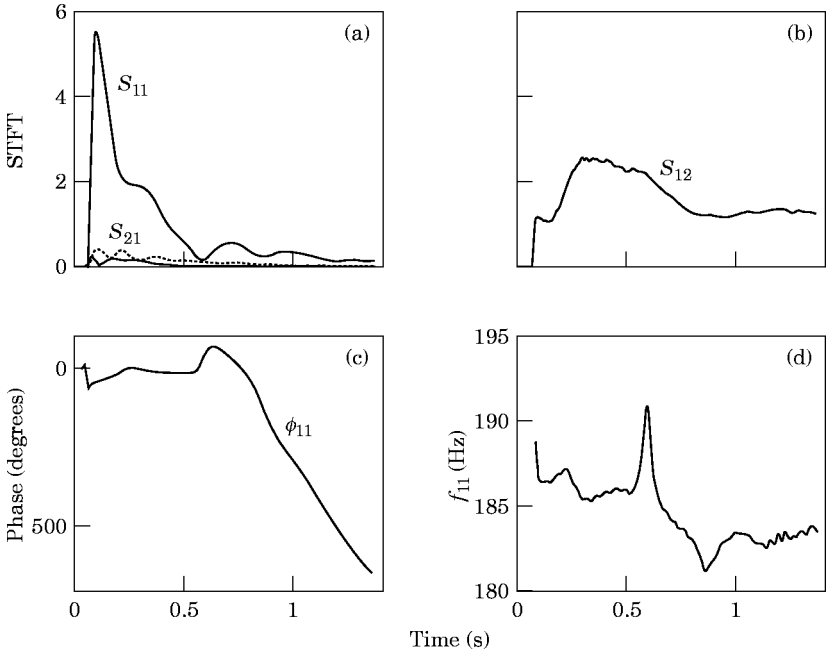

Figure 8. Experimental results for the double-second $\mathbf{F}_3^{\#}$ note played *forte* with skirt coupling: (a) note displacement STFT, ($\cdots$, S_{31}), (b) STFT of the skirt component (c) phase-time response of the first mode on the note, (d) frequency modulation on f_{11} (= 185·0 + $\phi'/2\pi$ Hz).

when it is possible to simultaneously excite dominant modes of nearly similar frequencies on the skirt that couple strongly to modes on the note.

The velocity STFT's were maximized at $f_{11} = 186$ Hz (mode 1) and $f_{21} = 374$ Hz (mode 2).

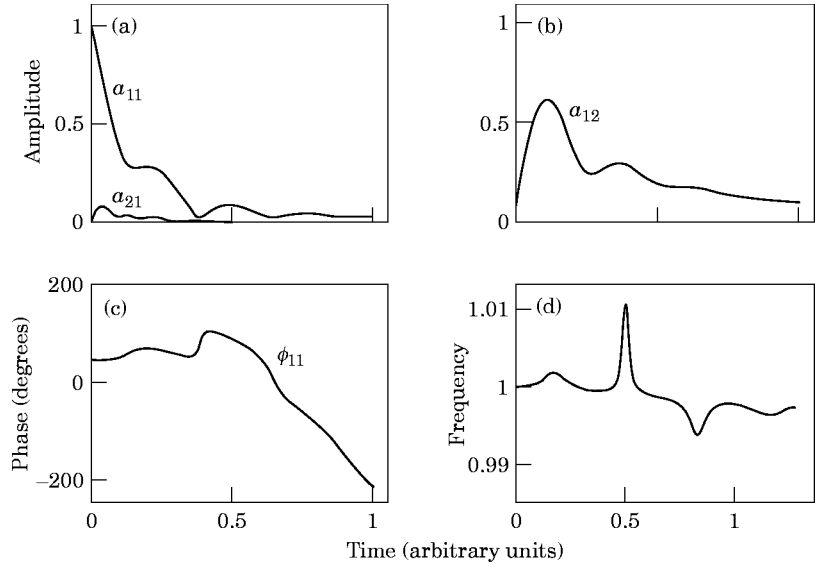

Figure 9. Analytical results for the simulated double-second $\mathbf{F}_3^{\#}$ note played *forte* with skirt coupling: (a) amplitudes of note components, (b) amplitude of skirt component (c) phase-time response of the first mode on the note, (d) frequency modulation on ω_{11} (= 1 + ϕ'_{11}).

This note-skirt system was modelled numerically and the results shown along with the frequency diagram in Figures 9(a–d). Modelling parameters were:

$\alpha_{211} = \alpha_{12} = 0{\cdot}001$, $\alpha_{112} = 0{\cdot}005$, $\alpha_{123} = \alpha_{213} = 0{\cdot}001$, $\alpha_{132} = \alpha_{312} = 0{\cdot}001$, $\alpha_{231} = \alpha_{321} = 0{\cdot}001$, all $\beta = 0{\cdot}0$, $\Gamma_{12}^{\{11\}} = 0{\cdot}0016$, $\Gamma_{11}^{\{12\}} = 0{\cdot}0033$, $\mu_{11} = \mu_{21} = \mu_{31} = 0{\cdot}001$, $\mu_{12} = 0{\cdot}0003$ $\sigma_1 = -0{\cdot}01$, $\sigma_2 = -0{\cdot}003$, $\sigma_3 = -0{\cdot}01$. Initial amplitudes were, *forte* level: $a_{11} = 1$, $a_{21} = a_{31} = 0$, $a_{12} = 0{\cdot}0$.

The good agreement between Figure 8 and Figure 9 confirms the applicability of the present theory to the coupled note-skirt system on the steelpan. The strength of the note-skirt coupling is determined by the values for $\Gamma_{jd}^{\{nd\}}$. While the values used here for these coupling coefficients (0·0016 and 0·0033) are somewhat smaller than those for the $\mathbf{D}_3$ note-skirt coupling on the bass (0.003 and 0·004, respectively) it should be noted that the coupled modes in the present example are closer in frequency (186 Hz and 183 Hz) than the coupled modes are on the bass (147 Hz and 179 Hz). The partials remained strong on the $\mathbf{D}_3$ bass note while the partials were almost insignificant on the $\mathbf{F}_3^{\#}$ double-second note.

4.4. COUPLING OF THE A_4 AND A_5 TENOR NOTES

On the tenor steelpan tested, the $\mathbf{A}_4$ (440·0 Hz) note which is an outer note was tuned by the panmaker to couple strongly to the $\mathbf{A}_5$ (880·0 Hz) inner note. The two notes act as a lower-octave-upper-octave sympathetic pair. The tone structures for the $\mathbf{A}_4$ note played *mezzo forte* (moderately loud) are shown in Figure 10(a) (the velocity time-history) and in Figure 10(c) (the STFT amplitude profile). Figure 10(c) shows an initially rapidly

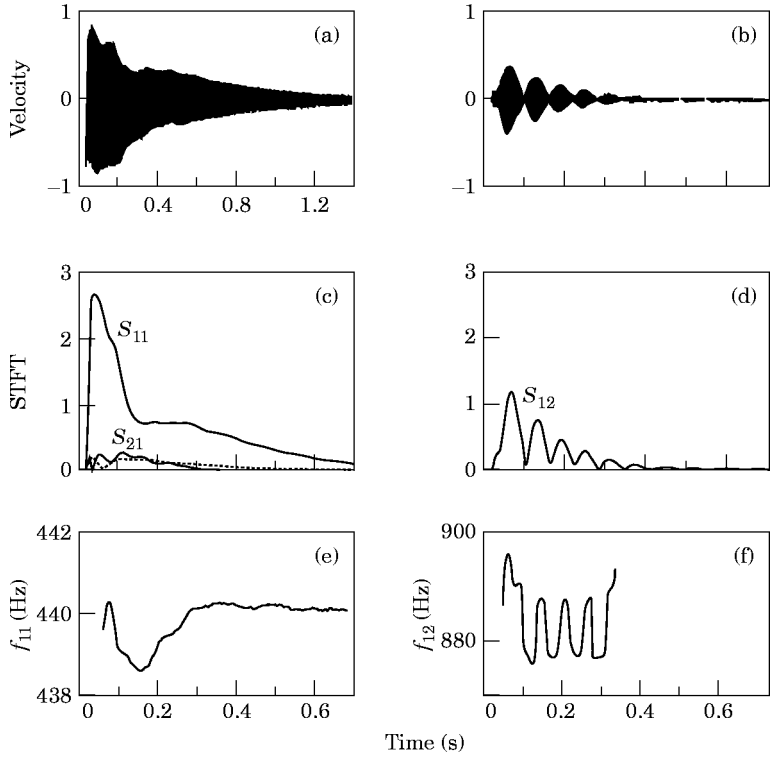

Figure 10. Comparison of experimental results for the coupled $\mathbf{A}_4$ and $\mathbf{A}_5$ notes on the tenor pan when $\mathbf{A}_4$ is played *forte*: (a) $\mathbf{A}_4$ velocity time-history, (b) $\mathbf{A}_5$ velocity time-history, (c) STFT of $\mathbf{A}_4$ components, ($\cdots$, S_{31}), (d) STFT of $\mathbf{A}_5$ component, (e) modulation of $\mathbf{f}_{11}$ ($= 440{\cdot}0 + \phi'/2\pi$ Hz), (f) modulation on f_{12} ($= 881{\cdot}0 + \phi'/2\pi$ Hz).

decaying amplitude profile followed by a period of almost constant amplitude, then by a period of slow decay. The frequency modulation accompanying these amplitude changes is shown in Figure 10(e). Notice the initial fall and rise in frequency immediately after impact.

The corresponding structures for the $\mathbf{A}_5$ note as it responds to the impact on the $\mathbf{A}_4$ note (Figures 10(b), 10(d) and 10(f)), show a strongly modulated 880 Hz component. These strong modulations are often observed for sympathetic pairs. STFT's were maximized at $f_{11} = 440$ Hz and $f_{12} = 881$ Hz.

The interaction process can be understood from the numerically modelled system, the results for which are shown in Figure 11. The numerical model reproduces the main amplitude and frequency modulations observed on the real system (compare Figures 10 and 11). The amplitude modulations clearly show the continuous exchange of energy between the two notes. The main channel for energy transfer from $\mathbf{A}_4$ to $\mathbf{A}_5$ is through the term $-(\beta^{\{12\}}_{11,11}/4\omega_{12})a_{11}^2 \sin(\gamma_1 + \gamma_3 + \theta_\beta)$ in equation (5g). This represents a non-linear (quadratic) coupling of the fundamental on the $\mathbf{A}_4$ note to the fundamental on the $\mathbf{A}_5$ note. The reverse coupling of these two modes is through the term $+(\beta^{\{11\}}_{12,11}/4\omega_{11})a_{12}a_{11} \sin(\gamma_1 + \gamma_3 + \theta_\beta)$. The periodicity of these two non-linear terms depend on the detuning parameter σ_3. The frequency modulations on these two modes are similarly accounted for by the terms containing $\beta^{\{11\}}_{12,11}$ and $\beta^{\{12\}}_{11,11}$ in equations (5d) and (5i), respectively. The frequency modulations are more pronounced on the model (Figures 11(c) and 11(d)) than they are on the real note (Figures 10(e) and 10(f)). Modelling parameters were, for the $\mathbf{A}_4$ note (domain 1):

$\alpha_{211} = \alpha_{121} = 0{\cdot}065$, $\alpha_{112} = 0{\cdot}03$, $\alpha_{123} = \alpha_{213} = 0{\cdot}06$, $\alpha_{132} = \alpha_{312} = 0{\cdot}001$, $\alpha_{231} = \alpha_{321} = 0{\cdot}03$, $\mu_{11} = 0{\cdot}0008$, $\mu_{21} = 0{\cdot}005$, $\mu_{31} = 0{\cdot}002$, $\sigma_1 = \sigma_2 = 0{\cdot}003$ $\beta^{\{11\}}_{12,11} = 0{\cdot}02$, all other $\beta = 0{\cdot}001$, $\Gamma^{\{21\}}_{12} = 0{\cdot}012$. Initial amplitudes were $a_{11} = 0{\cdot}65$, $a_{21} = a_{31} = 0$.

For the $\mathbf{A}_5$ note (domain 2), the parameters were:

$\alpha_{211} = \alpha_{121} = 0{\cdot}001$, $\alpha_{112} = 0{\cdot}001$, $\mu_{12} = 0{\cdot}0008$, $\mu_{22} = 0{\cdot}0008$, $\sigma_3 = 0{\cdot}03$, $\sigma_4 = 0{\cdot}001$, $\beta^{\{12\}}_{11,11} = 0{\cdot}12$, all other $\beta = 0{\cdot}001$, $\Gamma^{\{12\}}_{21} = 0{\cdot}06$; initial amplitudes were $a_{12} = 0{\cdot}02$, $a_{22} = 0$.

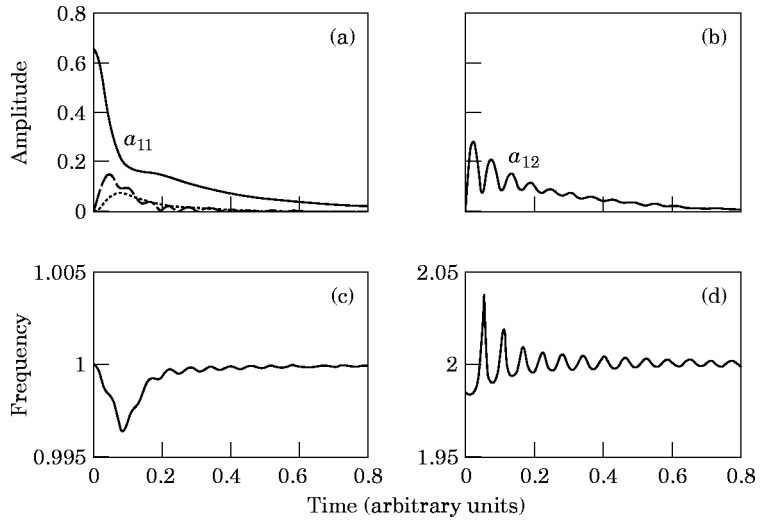

Figure 11. Comparison of analytical results for the coupled $\mathbf{A}_4$ and $\mathbf{A}_5$ notes on the simulated tenor pan when $\mathbf{A}_4$ is played *forte*: (a) amplitudes of $\mathbf{A}_4$ components, (— —, a_{21}; · · · · ·, a_{31}), (d) amplitude of $\mathbf{A}_5$ component, (e) modulation on ω_{11} (= 1 + ϕ'_{11}), (f) modulation on ω_{12} (= 2 + ϕ'_{12}).

5. CONCLUSION

The motion of the coupled note-note or note-skirt system retains some of the characteristics of the single note dynamical system, as expected, when the coupling coefficients are small or when the mode frequencies are not closely related harmonically. The modulation characteristics of the moderately or strongly coupled systems are quite different from those of the uncoupled system. Unique tonal qualities are obtained on note pairs in sympathetic vibration with the upper octave often showing deep amplitude and frequency modulations.

REFERENCES

1. A. Achong 1996 *Journal of Sound and Vibration* **197**, 471–487. The steelpan as a system of non-linear mode-localized oscillators, Part I: Theory, simulations, experiments and bifurcations.
2. A. Achong 1996 *Journal of Sound and Vibration* **191**, 207–217. Vibrational analysis of mass loaded plates and shells by the receptance method with application to the steelpan.
3. A. H. Nayfeh and D. T. Mook 1979 *Nonlinear Oscillations*. Wiley-Interscience.
4. A. H. Nayfeh 1983 *Journal of Sound and Vibration* **90**, 237–244. The response of multi-degree-of-freedom systems with quadratic non-linearities to a harmonic parametric resonance.